Article

Cell Chemical Biology

Aggregation and Its Influence on the Immunomodulatory Activity of Synthetic Innate Defense Regulator Peptides

Graphical Abstract

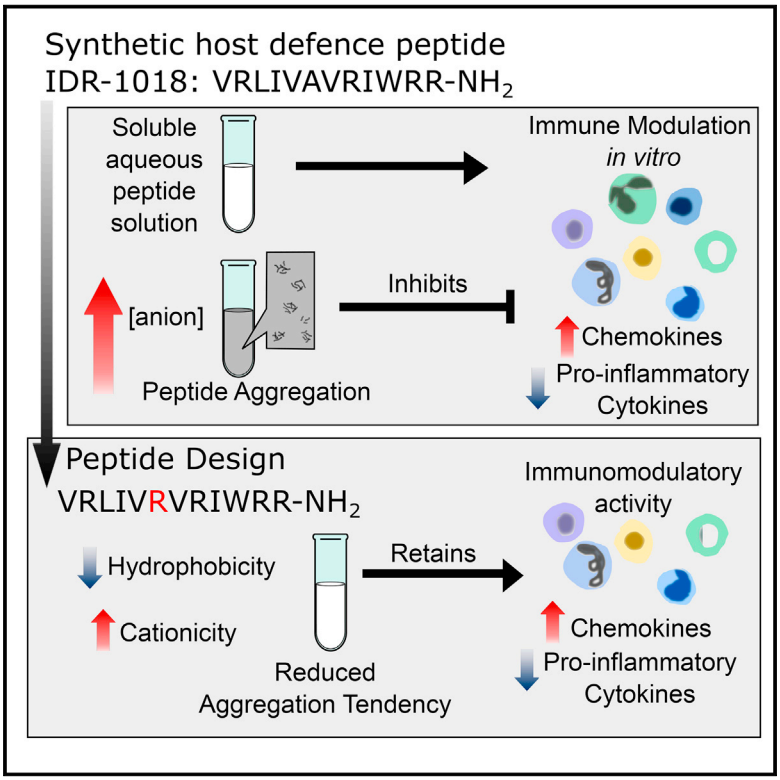

Highlights

- Aggregation of IDR-1018, a synthetic host defense peptide, is salt dependent
- Peptide aggregation reduced the immunomodulatory activity of IDR-1018 *in vitro*
- Derivatives were designed to reduce aggregation while retaining biological activity
- Aggregation must be considered when designing synthetic peptide therapeutics

Authors

Evan F. Haney, Bing (Catherine) Wu, Kelsey Lee, Ashley L. Hilchie, Robert E.W. Hancock

Correspondence

bob@hancocklab.com

In Brief

Haney et al. characterize the salt-dependent aggregation property of IDR-1018, a synthetic host defense peptide, and demonstrate that aggregation negatively influences immunomodulatory activity of synthetic peptides *in vitro*. Derivatives are then designed with reduced aggregation tendencies but retained immunomodulatory functions.

Haney et al., 2017, Cell Chemical Biology *24*, 969–980
August 17, 2017
http://dx.doi.org/10.1016/j.chembiol.2017.07.010

CellPress

Cell Chemical Biology
Article

Aggregation and Its Influence on the Immunomodulatory Activity of Synthetic Innate Defense Regulator Peptides

Evan F. Haney,[1] Bing (Catherine) Wu,[1] Kelsey Lee,[1] Ashley L. Hilchie,[1] and Robert E.W. Hancock[1,2,*]
[1]Center for Microbial Diseases and Immunity Research, Department of Microbiology and Immunology, University of British Columbia, #232, 2259 Lower Mall Research Station, Vancouver, BC V6T 1Z4, Canada
[2]Lead Contact
*Correspondence: bob@hancocklab.com
http://dx.doi.org/10.1016/j.chembiol.2017.07.010

SUMMARY

There is increasing interest in developing cationic host defense peptides (HDPs) and their synthetic derivatives as antimicrobial, immunomodulatory, and anti-biofilm agents. These activities are often evaluated without considering biologically relevant concentrations of salts or serum; furthermore certain HDPs have been shown to aggregate *in vitro*. Here we examined the effect of aggregation on the immunomodulatory activity of a synthetic innate defense regulator peptide, 1018 (VRLIVAVRIWRR-NH_2). A variety of salts and solutes were screened to determine their influence on 1018 aggregation, revealing that this peptide "salts out" of solution in an anion-specific and concentration-dependent manner. Furthermore, the immunomodulatory activity of 1018 was found to be inhibited under aggregation-promoting conditions. A series of 1018 derivatives were synthesized with the goal of disrupting this self-assembly process. Indeed, some derivatives exhibited reduced aggregation while maintaining certain immunomodulatory functions, demonstrating that it is possible to engineer optimized synthetic HDPs to avoid unwanted peptide aggregation.

INTRODUCTION

Natural and synthetic peptides have been studied as potential sources for new antibiotics for many years, and the immunomodulatory and antibiofilm activities of many host defense peptides (HDPs; also termed antimicrobial peptides) has recently gained significant attention (Hancock et al., 2016). Antimicrobial, immunomodulatory, and antibiofilm peptides share many structural characteristics, such as overall cationic charge and a high proportion of hydrophobic residues (Nguyen et al., 2011). These physicochemical properties permit HDPs to adopt amphipathic structures in the presence of biological membranes, which is important for their overall mechanisms of action (Fjell et al., 2012; Mookherjee et al., 2009). However, despite this sustained interest in developing and optimizing synthetic HDPs for therapeutic applications, very few sequences have emerged as viable drug candidates. One reason for this is that many protein-based drugs have a strong tendency to aggregate, which can lead to decreased potency, stability, and/or increased toxicity (Frokjaer and Otzen, 2005).

Peptide aggregation is a complex process known to be influenced by a number of fundamental characteristics such as secondary structure, hydrophobicity, and charge, as well as the composition and concentration of solutes in the surrounding environment (Roberts, 2014). A variety of natural HDPs, including LL-37, α-defensins, and dermaseptin (Auvynet et al., 2008; Horn et al., 2012; Li et al., 2007), oligomerize or precipitate at critical concentrations in various solutions. Peptide aggregation has been shown to decrease the antimicrobial potency of peptides and peptidomimetics (Sarig et al., 2008) and may even contribute to enhanced toxicity (Ghosh et al., 1997). Therefore, it is imperative to evaluate the aggregation tendency of novel innate defense regulator (IDR) peptides at early stages of development and to mitigate any aggregation tendency that would otherwise lead to the rejection of aggregation-prone peptides as potential therapeutics.

Protein aggregation is known to contribute to a variety of diseases (Aguzzi and O'Connor, 2010), and it is thought that protein aggregates are inherently toxic (Bucciantini et al., 2002); however, it is still unclear what role peptide aggregation plays in the biological activity of HDPs, particularly in the context of immune modulation. Delineating the aggregation property of synthetic IDR peptides is crucial for advancing potential drug candidates through to clinical applications. Any negative effects due to aggregation could potentially be overcome by a variety of tactics including sequence optimization (Chiti et al., 2003), use of small-molecule inhibitors (Doig and Derreumaux, 2015), or specific drug formulation strategies (Du and Stenzel, 2014) to counteract what might be a class effect of cationic amphipathic peptides.

IDR-1018 (also referred to as 1018) is a 12-residue (VRLIVAVRIWRR-NH_2) cationic polypeptide derived from the natural bovine peptide, bactenecin, which possesses a broad range of immunomodulatory properties (Pena et al., 2013; Wieczorek et al., 2010) and has been shown to offer protection in animal models of diverse bacterial infections, cerebral malaria, wound healing, and perinatal brain injury (Achtman et al., 2012; Bolouri et al., 2014; Steinstraesser et al., 2012). Although weakly active against planktonic cells as a direct antimicrobial, 1018

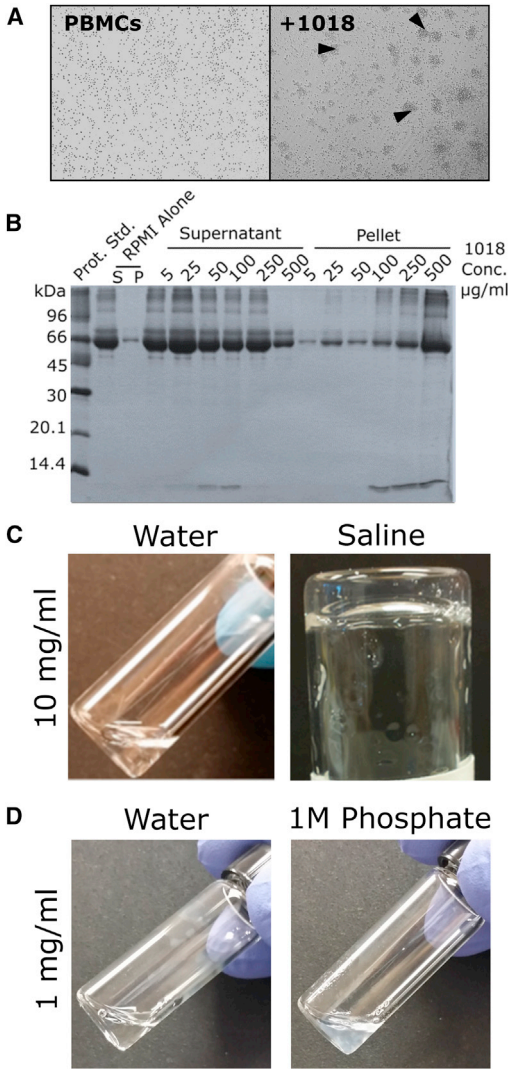

Figure 1. Aggregation Character of 1018

(A) Small aggregates interspersed among the cells (indicated by arrowheads) appeared when 1018 (50 μg/mL) was added to PBMCs in 10% RPMI.

(B) Peptide 1018 co-precipitated with serum proteins in 10% RPMI in a concentration-dependent manner as visualized by SDS-PAGE gel electrophoresis.

(C) When prepared at 10 mg/mL in water, 1018 remained in solution but formed a hydrogel in saline solution at the same concentration.

(D) Conversely, 1018 prepared at 1 mg/ml in 1 M sodium phosphate (pH 7.0) became turbid, indicative of peptide aggregation.

also inhibits the development of bacterial biofilms *in vitro* and eradicates preformed biofilms in a broad spectrum manner (de la Fuente-Núñez et al., 2014). This dual immunomodulatory and antibiofilm character makes 1018 an attractive drug candidate to be developed as a novel therapeutic to treat biofilm associated infections *in vivo* (Mansour et al., 2015). However, during our extensive testing of this peptide, it has become apparent that 1018 aggregates under various conditions, particularly at high concentrations and in tissue culture media.

Here, we sought to evaluate the salt-specific aggregation tendency of 1018 and aimed to characterize the effect of peptide aggregation on its immunomodulatory activities *in vitro*. Various aqueous solutions of salts and other dissolved solutes were screened to identify conditions that promoted 1018 aggregation. Once identified, we tested the effect of administering 1018 prepared in aggregation-free or aggregation-prone delivery vehicles on the *in vitro* immunomodulatory activity against peripheral blood mononuclear cells (PBMCs) as well as human bronchiolar epithelial (HBE) cells. To identify the region of the peptide responsible for this self-assembly character, a series of peptides were designed focusing on altering the largest hydrophobic stretch in 1018, as hydrophobic stretches are known to promote the formation of peptide aggregates (Kim and Hecht, 2006). This provided evidence that the hydrophobic stretch between Leu-3 and Val-7 in 1018 is responsible for the aggregation tendency of this peptide. We also demonstrate that 1018 derivatives can be rationally designed to reduce this aggregation character while retaining much of the immunomodulatory activity of the parent sequence. This study is the first to systematically assess the effect of peptide aggregation on the immunomodulatory activity of synthetic IDR peptides and demonstrates that it is possible to engineer peptides with potent immunomodulatory properties and low aggregation tendencies.

RESULTS

Characterization of 1018 Aggregation

Preliminary observations indicated that 1018 formed amorphous aggregates under tissue culture conditions (Figure 1A). To test whether these aggregates were composed of peptide alone or if serum proteins co-precipitated with peptide, increasing concentrations of 1018 were incubated in RPMI containing 10% fetal bovine serum (FBS) (10% RPMI) for 3 hr, and then the mixtures were centrifuged to pellet any aggregates. The resulting supernatants and pellets were subjected to SDS-PAGE analysis revealing that 1018 co-precipitated serum proteins in a concentration-dependent manner, with substantial aggregation of serum proteins at peptide concentrations above 100 μg/mL (Figure 1B). In addition, it was observed that solutions of 1018 exhibited different behaviors depending on the nature of the solute used to dissolve the peptide. For instance, 10 mg/mL stock solutions of 1018 in water remained soluble, while a solution at the same concentration prepared in sterile saline resulted in the formation of a hydrogel (Figure 1C). In addition, 1 mg/mL peptide solutions prepared in sodium phosphate solutions became turbid presumably due to the self-assembly of 1018 (Figure 1D). Altogether, these observations suggested that the propensity for 1018 to aggregate depended on the composition of the solution in which it was dissolved, and that its tendency to aggregate was influenced by the peptide concentration and the presence of dissolved ions and solutes.

Aggregation Behavior of 1018

To better understand the aggregation behavior of 1018, we screened 1 mg/mL solutions of 1018 prepared in the presence of different ions and solutes and looked for increases in sample turbidity as an indicator of peptide aggregation since large increases in turbidity correlated with the formation of visible polydisperse aggregates (Figure 1D). Compared with 1018 in water, we found that 1018 tended to aggregate in an

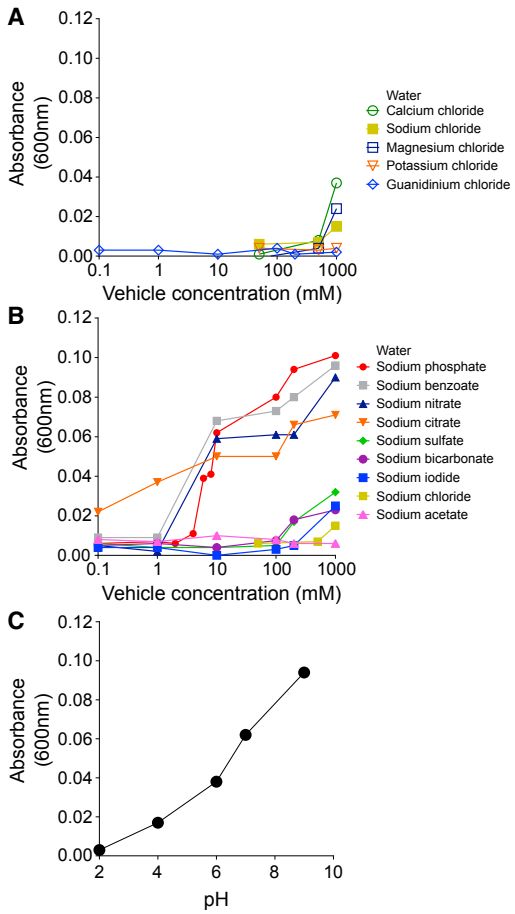

Figure 2. Effect of Salt and pH on 1018 Aggregation

(A and B) The aggregation of 1018 (1 mg/mL) was evaluated in the presence of chloride salts of various cations (A) while the influence of anions was evaluated by testing sodium salt forms (B).

(C) The aggregation tendency of 1018 in 25 mM sodium phosphate buffer was also found to be pH dependent. In all samples, an increase in turbidity at 600 nm was indicative of aggregation. See also Table S1 and Figure S1.

ion concentration-dependent manner in the presence of specific ions (Figure 2). In solutions where the anion was chloride and the cation was varied, namely sodium chloride, calcium chloride, magnesium chloride, or guanidinium chloride, no aggregation was observed below 500 mM, and only slight to moderate increases in sample turbidity were observed at salt concentrations of 1 M (Figure 2A). In contrast, the sodium salt forms of certain anions induced significant 1018 aggregation at concentrations as low as 10 mM. The strongest aggregation was observed in solutions containing large polyatomic anions, such as phosphate, benzoate, nitrate, and citrate (Figure 2B). A comparatively small amount of aggregation was observed in solutions containing sulfate and bicarbonate anions as well as chloride and iodide monoatomic anions, and only at ion concentrations above 200 mM. Interestingly, 1018 prepared in sodium acetate did not induce any appreciable aggregation, suggesting that this anion may provide an exception to the effect of large polyatomic anions on the aggregation property of synthetic peptides. The aggregation tendency of 1018 was also found to be pH dependent, with acidic phosphate solutions yielding lower turbidity measurements compared with basic solutions, likely due to the differences in the protonation state of the phosphate ions at each pH (Figure 2C). These results demonstrate that the aggregation tendency of 1018 was largely influenced by the presence and concentration of anions, as well as the overall strength of the negative charge in solution. A number of other solutions were screened for their ability to induce 1018 aggregation, including various buffers, sugars, and amino acids (Table S1), but none of these conditions caused noticeable aggregation of 1018 (Figure S1).

Effect of Aggregation on Immunomodulatory Activity

To evaluate the effect of aggregation on the immunomodulatory activity of 1018, we prepared 1 mg/mL stock solutions of 1018 in five different delivery vehicles: water, sterile saline, tissue culture media (10% RPMI for PBMCs or minimum essential medium [MEM] with 1% FBS for HBEs, respectively), 200 mM sodium nitrate ($NaNO_3$), or 200 mM sodium sulfate (Na_2SO_4). Additional peptide samples containing phosphate ions were prepared either in sterile PBS or 200 mM sodium phosphate (NaH_2PO_4) adjusted to a pH of 7.0. Based on the results from the aggregation screen (Figure 2), peptide solutions with high concentrations of ions were expected to promote aggregation, whereas weakly ionic solutions should allow 1018 to remain soluble. Indeed, this was the case as 1 mg/mL stock solutions of 1018 in water and saline remained clear, whereas 200 mM nitrate and sulfate samples exhibited increased peptide aggregation, and stock solutions prepared in 10% RPMI or 1% MEM caused a substantial increase in sample turbidity (Figure 3A). Interestingly, when added to PBMCs, distinct aggregation patterns were observed for each stock solution of 1018, particularly at the highest tested peptide concentration of 50 μg/mL (Figure 3B). In samples containing 1018 delivered in water or saline, irregularly sized and shaped aggregates, consisting of cells and amorphous protein aggregates, were distributed throughout the well. In samples treated with 1018 prepared in 10% RPMI, a large mat of aggregated material, likely consisting of complexes of 1018 with serum proteins, could be seen throughout the treatment well. In samples containing 200 mM sodium nitrate or sulfate, large crystalline aggregates were observed throughout the well (Figure 3B). Similar 1018 aggregation profiles were seen for HBE samples, and in all cases the aggregation patterns were unaffected by the presence of bacterial lipopolysaccharide (LPS) or polyinosinic:polycytidylic acid (poly(I:C)) (not shown).

When delivered from a 1 mg/mL stock solution prepared in water, 1018 was relatively non-toxic toward PBMCs and HBEs, since concentrations of peptide of $\leq$50 μg/mL induced less than ~10% toxicity according to the LDH release assay (Figures 3C and 3D). Treatment with 1018 alone resulted in a concentration-dependent production of monocyte chemoattractant protein-1 (MCP-1) and interleukin-8 (IL-8) chemokines from PBMCs and HBEs, respectively (Figures 3E and 3F). In addition, 1018 suppressed the production of pro-inflammatory cytokines from cells stimulated with TLR agonists. Specifically, 1018 suppressed the production of IL-1β from LPS-stimulated PBMCs and reduced IL-6 production from HBEs stimulated with poly(I:C) (Figures 3G and 3H). Similar immunomodulatory results were seen in samples treated with a 1018 stock solution prepared in

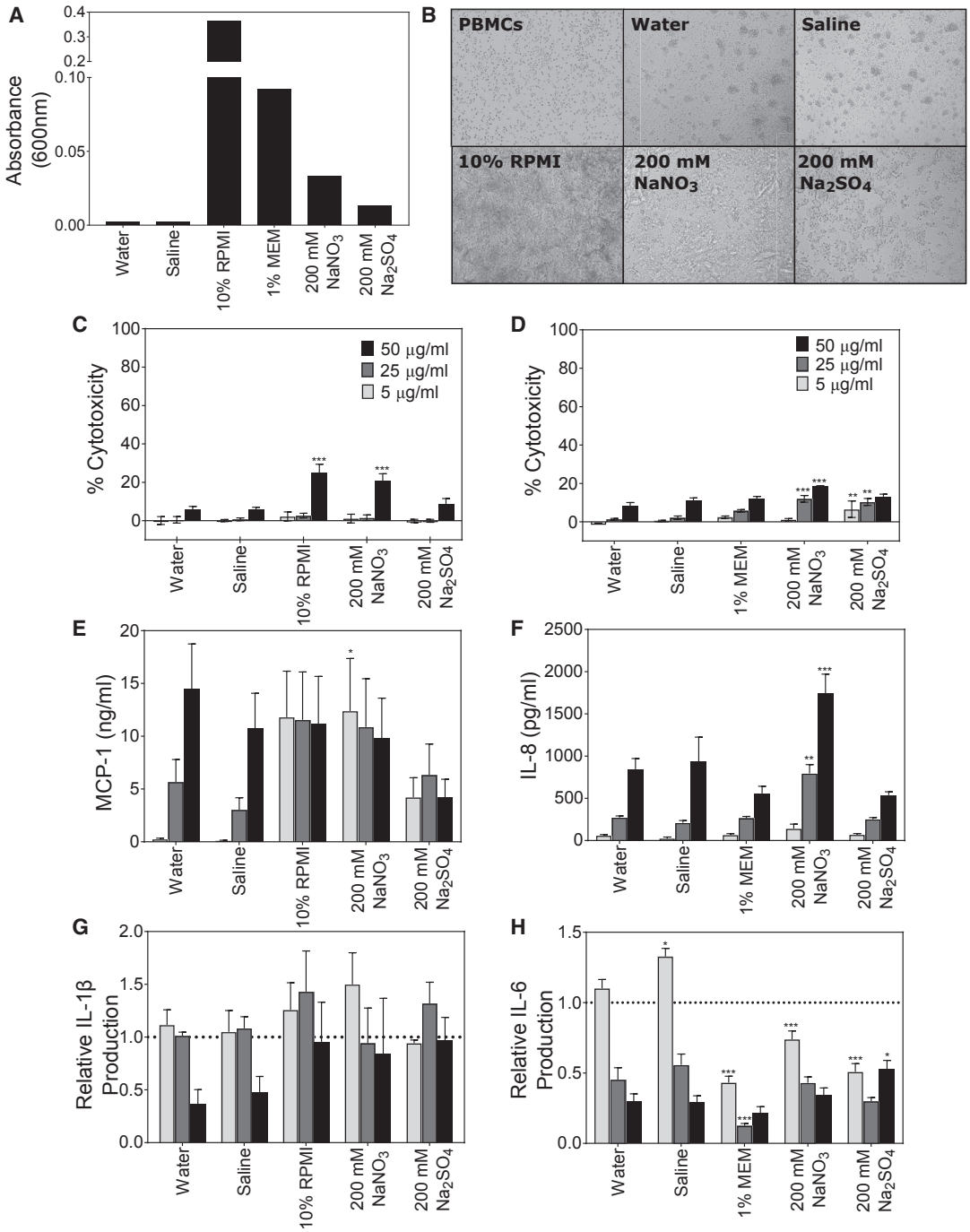

Figure 3. Effect of 1018 Aggregation on Cytotoxicity and Immunomodulatory Activity

(A and B) Aggregation tendency of 1 mg/mL 1018 stock solutions before (A) and after (B) delivery to tissue culture media. Representative microscopy images of 1018 added to PBMCs at 50 μg/mL from 1 mg/mL stock solutions prepared in the indicated delivery vehicles. Biological activities were measured at peptide concentrations of 50 (black), 25 (dark gray), and 5 μg/mL (light gray).

(C–F) Cytotoxicity was measured against PBMCs (C) and HBEs (D) using the LDH assay. Chemokine induction by 1018 was evaluated specifically looking at MCP-1 production from PBMCs (E) and IL-8 production from HBEs (F). The amount of chemokine induced by vehicle alone has been subtracted in the final analysis.

(G and H) The suppression of pro-inflammatory cytokine production by 1018 was assessed by measuring the amount of IL-1β produced by LPS-stimulated PBMCs (G) or IL-6 produced by poly(I:C)-stimulated HBEs (H). In these cases, the response has been normalized to the amount of cytokine induced by the TLR agonist for each vehicle control condition, defined as 1.

Data shown are mean ± SEM. Statistical significance was calculated using a two-way ANOVA with a Bonferroni correction comparing each derivative peptide treatment condition to the corresponding concentration of 1018. *$p \leq 0.05$, **$p \leq 0.01$, and ***$p \leq 0.001$. See also Figures S2 and S3.

saline, suggesting that both these vehicles allowed the peptide to be delivered in an unaggregated state.

Solutions that promoted 1018 aggregation prior to delivery to cells significantly affected the biological activity profile of the peptide, consistent with the hypothesis that the aggregation state of 1018 influenced the toxicity and immunomodulatory activity of this peptide *in vitro*. For example, 1018 delivered in 10% RPMI or 200 mM solutions of sodium nitrate or sulfate was more toxic (up to 30% LDH release) toward both PBMCs and HBEs (Figures 3C and 3D). Some of these aggregation-prone conditions also caused enhanced MCP-1 production from PBMCs at peptide concentrations of 25 and 5 μg/mL, particularly for the 10% RPMI and nitrate samples (Figure 3E). For HBEs, significantly increased cytotoxicity was observed for samples in which peptide was delivered in solutions containing high concentrations of nitrates and sulfates (Figure 3D). However, the levels of IL-8 produced by HBEs were largely unaffected, and only 1018 delivered from a 200 mM nitrate solution significantly increased production of IL-8 from HBEs (Figure 3F). Taken together, this suggests that aggregation-prone conditions may place additional stress on cells *in vitro*, leading to enhanced LDH release and, likely due to activation of stress-induced MAP kinase pathways, increased chemokine production in monocytes. In terms of suppression of pro-inflammatory cytokines, all aggregation-promoting delivery vehicles completely abolished the IL-1β-suppressing ability of 1018 when added to LPS-stimulated PBMCs (Figure 3G). Interestingly, many of the 1018 aggregation-prone solutions still suppressed the IL-6 response from poly(I:C)-stimulated HBEs (Figure 3H), although it should be noted that the vehicle treatments alone had a suppressive effect on IL-6 production from poly(I:C)-stimulated HBE cells (Figure S2), indicating that some of this suppressive effect may be due to an effect of the delivery vehicle alone.

Phosphate-containing delivery vehicles were also tested for delivery of 1018 since phosphate is commonly used as a buffering agent and PBS is commonly used as a non-toxic, isotonic solution for drug delivery. The aggregation pattern of 1018 prepared in PBS was similar to that seen in water, while 1018 delivered in 200 mM sodium phosphate solutions was similar to those seen for the stock solutions prepared in nitrates and sulfates (Figures S3A and S3B). However, in both cases, the immunomodulatory activity was substantially muted compared with the peptide delivered in water (Figures S3C–S3H). Curiously, both of the phosphate-containing delivery vehicles enhanced the toxicity of the peptide toward PBMCs, suggesting that the phosphate ions and peptide form a complex that is more toxic to cells. In addition, treatment of HBEs with 200 mM NaH_2PO_4 alone proved to be toxic (Figure S2), which made interpretation of the HBE immunomodulatory activity data difficult and may account for chemokine and cytokine production in these samples. Taken together, we recommend that phosphate-containing buffers be avoided as delivery vehicles for peptides.

Overall, based on the results of this delivery vehicle screen, it is clear that the aggregation state of 1018 significantly influences the biological activity of the peptide *in vitro.* This property could have implications for future development of this peptide as a chemotherapeutic agent. Therefore, in an attempt to overcome this issue, a series of 1018 derivatives were designed with the aim of mitigating the aggregation propensity. The aggregation tendency and biological characterization of these 1018 derivatives is described below.

Engineering Out the Aggregation Property of 1018

Two other IDR peptides with similar sequences to 1018, IDR-1002 (VQRWLIVWRIRK-NH_2) and IDR-HH2 (VQLRIRVAVIRA-NH_2), for which immunomodulatory activities have been characterized both *in vitro* (Niyonsaba et al., 2013) and *in vivo* (Nijnik et al., 2010; Rivas-Santiago et al., 2013), were found to have distinct salt-specific aggregation properties compared with 1018 (Figure S4). This observation suggested to us that the "salting out" effect is largely influenced by the peptide sequence and that it therefore may be possible to engineer out the unfavorable aggregation tendency while retaining potent immunomodulatory activity.

Based on previous studies that indicated that peptide aggregation was favored by short sequence segments of 5–15 hydrophobic residues (Baets et al., 2014), we proposed that the aggregation propensity of 1018 could be attributed to the stretch of the five hydrophobic residues between Leu-3 and Val-7. Therefore, a series of 1018 derivatives were synthesized in which the hydrophobic patch was disrupted to assess the influence of this region on the aggregation propensity of 1018 (Table 1). Using this approach, three derivatives were synthesized, wherein the hydrophobic patch was deleted completely (1101, Δ3-7), replaced by a single Phe residue (1102, Δ3-7+F) or shortened by removing the two most hydrophobic residues, Leu-3 and Ile-4 (1103, Δ3-4). Two more peptides focused on the largest hydrophobic residue in the center of the hydrophobic patch, Val-5. One peptide replaced Val-5 with a Pro residue (1104, V5P) as proline residues are known to break secondary structural elements (Richardson and Richardson, 1989) and have been shown to inhibit aggregation of amyloid β peptides (Morimoto et al., 2002). The other designed peptide introduced a cationic Arg at position 5 (1105, V5R) to reduce the overall hydrophobicity in this region. In agreement with the predicted aggregation propensities (Table 1), all peptides with disrupted hydrophobic patches (1101–1105) showed decreased aggregation in the presence of phosphate ions compared with 1018 (Figure 4A), supporting the hypothesis that this hydrophobic patch is largely responsible for the aggregation character of 1018.

The immunomodulatory and cytotoxic activity of these 1018 derivatives was evaluated *in vitro* as described above. To allow for comparison between peptides, the concentrations were normalized to the equivalent molar concentrations of 1018 tested in previous experiments (i.e., 50, 25, and 5 μg/mL, which corresponds to 32.5, 16.3, and 3.25 μM). While none of these 1018 derivatives (1101–1105) resulted in enhanced cytotoxicity toward PBMCs or HBEs (Figures 4B and 4C), all of these derivatives proved to be largely inactive as immunomodulatory peptides. Specifically, none of the five peptides induced MCP-1 production or suppressed LPS-induced IL-1β pro-inflammatory cytokine production from PBMCs (Figures 4D and 4F). Moreover, compared with 1018-treated cells, peptide-mediated IL-8 production, as well as the suppression of poly(I:C)-induced IL-6 production from HBEs, was substantially muted (Figures 4D and 4E). These results demonstrate the importance of this stretch of amino acids for the biological activity of 1018 and highlight the difficulties associated with manipulating peptide sequences for a specific biophysical properties, since this

Table 1. IDR-1018 Derivatives Disrupting the Hydrophobic Patch between L^3IVAV^7 (1101–1105) or Designed to Decrease Aggregation Propensity (2001–2008)

Peptide Name	Modification	Sequence	Net Charge	Aggregation Propensity
1018	–	VRLIVAVRIWRR-NH_2	5	0.487
1101	Δ3-7	VRRIWRR-NH_2	5	−0.072
1102	Δ3-7 + F	VR**F**RIWRR-NH_2	5	0.156
1103	Δ3-4	VRVAVRIWRR-NH_2	5	0.264
1104	V5P	VRLI**P**AVRIWRR-NH_2	5	0.327
1105	V5R	VRLI**R**AVRIWRR-NH_2	6	0.251
2001	A6K	VRLIV**K**VRIWRR-NH_2	6	0.413
2002	W10R	VRLIVAVRI**R**RR-NH_2	6	0.298
2003	A6K, W10R	VRLIV**K**VRI**R**RR-NH_2	7	0.223
2004	L3V, A6K, W10R	VR**V**IV**K**VRI**R**RR-NH_2	7	0.241
2005	A6R	VRLIV**R**VRIWRR-NH_2	6	0.387
2006	L3W, A6K, W10R	VR**W**IV**K**VRI**R**RR-NH_2	7	0.194
2007	V1R, A6K	**R**RLIV**K**VRIWRR-NH_2	7	0.177
2008	V1R, L3W, A6K, W10R	**R**R**W**IV**K**VRI**R**RR-NH_2	8	−0.042

Residues that have been changed compared with 1018 are highlighted in bold. The aggregation propensities of each peptide was calculated by AGGRESCAN (Conchillo-Solé et al., 2007). The value indicated is the average of the amino acid aggregation-propensity value (a^3v) across the length of the input sequence. Note that the amidated C terminus was not considered as an input parameter for the AGGRESCAN calculation. See also Figure S6.

can have a negative impact on the biological activity of the peptide.

To overcome this challenge, a second series of peptides were rationally designed using sequence information derived from a screen of 1018 single amino acid substitutions variants that were synthesized on cellulose membranes. Such a strategy has previously been used to generate optimized derivatives of IDR-1002 and IDR-HH2 (Haney et al., 2015). A total of 96 variants were generated in which each amino acid in 1018 was individually substituted with one of nine amino acids (R, K, Q, G, A, W, V, L, or I), and all of these derivatives were screened for their ability to induce MCP-1 from PBMCs. A large distribution in the chemokine-inducing abilities of all the peptides was observed among the variants (Figure 5A), revealing that even a small change in a peptide sequence can have a dramatic influence on the biological activity. When plotted as a substitution matrix across the length of the 1018 sequence, residues that were essential for the MCP-1 induction activity and could be mutated without sacrificing the biological activity became apparent (Figure 5B). For example, Arg-8 in 1018 can only be mutated to a Lys to preserve the chemokine-inducing activity while all other substitutions at this position dramatically reduced this activity. Conversely, Ala-6 can tolerate multiple amino acid substitutions as many of these 1018 derivatives retain much of the activity of the parent peptide (i.e., they appear red or white in the substitution matrix). Using this matrix as a guide, we designed 1018 derivatives that combined favorable mutations, which should enhance or retain MCP-1 production from PBMCs while also decreasing the predicted aggregation propensity. In total, eight derivatives were synthesized (2001–2008) focusing primarily on substituting the hydrophobic residues at positions 1, 6, and 10 with cationic residues (Table 1).

The ''salting out'' tendencies of the designed 1018 derivatives were evaluated at increasing concentrations of phosphate ions revealing that all of these peptides exhibited some level of phosphate-induced aggregation (Figure 6A). Importantly, compared with 1018, most peptides showed decreased turbidity in 10 mM phosphate, suggesting that these sequence manipulations successfully reduced the peptide aggregation tendencies. Three sequences in particular, 2002, 2007, and 2008, exhibited decreased self-association tendencies at phosphate concentrations as high as 100 mM. We also evaluated the tendency of these peptides to co-precipitate serum proteins from 10% RPMI, revealing that only 2001 and 2005 aggregated with serum proteins at a peptide concentration of 0.5 mg/mL (Figure 6B). Interestingly, these two peptides were similar in that they both replaced Ala-6 in 1018 with a cationic residue (Lys in 2001 or Arg in 2005), and they were predicted to be the most aggregation prone of the rationally designed 1018 derivatives (Table 1).

All of the 1018 derived peptides, 2001–2008, exhibited immunomodulatory activity; however, in many cases, the levels of peptide-mediated chemokine induction and pro-inflammatory cytokine suppression were altered compared with the effects caused by 1018. Five of these derivatives, namely 2001, 2003, 2004, 2006, and 2008, proved to be significantly more toxic toward both PBMCs and HBEs (Figures 6C and 6D). Therefore, an unexpected consequence of optimizing some peptides for chemokine induction was an undesired increase in peptide cytotoxicity. The complete biological activity profiles of peptides 2001–2008 are presented in Figure S5.

Analysis of the MCP1-1 levels produced by PBMCs in response to the three non-toxic peptides (2002, 2005, and 2007) revealed that many of these derivatives enhanced chemokine production compared with 1018 (Figure 6E). Treatment of PBMCs with 32.5 μM of 2002, 2005, and 2007 all led to higher levels of MCP-1 compared with the same concentration of 1018, and 2005 in particular caused pronounced increases at every peptide concentration tested. Interestingly, only peptide 2005 retained the IL-8-stimulating properties of the parent sequence against HBE cells, while 2002 and 2007 led to reduced levels of IL-8 induction by 1018 at 32.5 μM (Figure 6F).

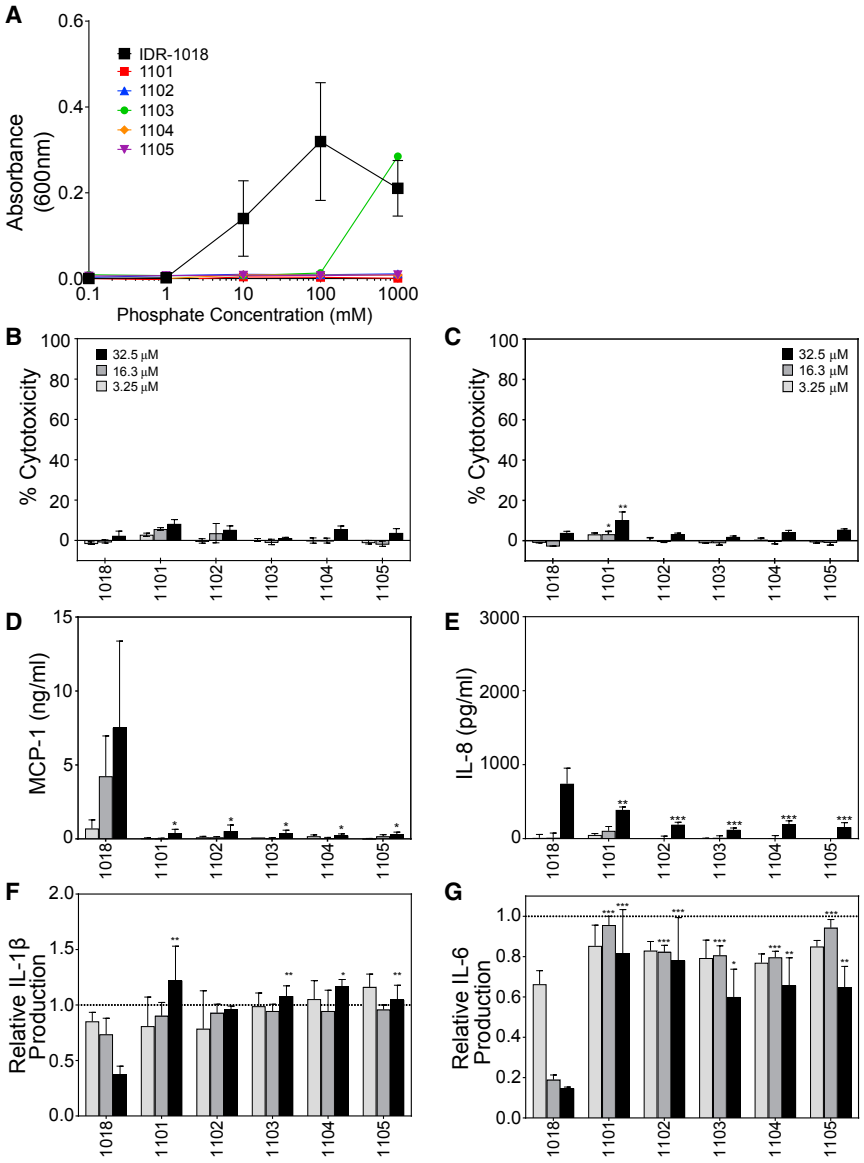

Figure 4. Activity of 1018 Derivatives Targeting Residues in the Hydrophobic Region, L^3IVAV^7

(A) Aggregation was evaluated by measuring the increase in sample turbidity at 600 nm of 1 mg/mL peptide solution prepared in increasing concentrations of sodium phosphate. Peptide activity was assessed at molar concentrations of 32.5 (black), 16.25 (dark gray), and 3.25 μM (light gray), corresponding to 1018 concentrations of 50, 25, and 5 μg/mL. The absorbance values for the 1018 samples represent the average of five individual measurements (±SD)

(B and C) Peptide cytotoxicity was evaluated against PBMCs (B) and HBEs (C) by the LDH release assay.

(D and E) Peptide-induced chemokine production of MCP-1 from PBMCs (D) or IL-8 from HBEs (E) was measured by ELISA.

(F and G) In addition, the peptide-mediated suppression of the pro-inflammatory cytokines IL-1β from LPS-stimulated PBMCs (F) or IL-6 from poly(I:C)-stimulated HBEs (G) was quantified and compared with the response of stimulated cells in the absence of peptide (defined as 1).

Data shown are mean ± SEM. Statistical significance was calculated using a two-way ANOVA with a Bonferroni correction comparing each derivative peptide treatment condition to the corresponding concentration of 1018. *$p \leq 0.05$, **$p \leq 0.01$, and ***$p \leq 0.001$. See also Figures S4 and S6.

DISCUSSION

The role of protein aggregation in diseases such as Alzheimer's disease, amyotropic lateral sclerosis, and other amyloidosis, as well as prion diseases, is well established (Aguzzi and O'Connor, 2010). In these cases, protein aggregation is directly related to disease progression, and identifying inhibitors of this aggregation to treat or eliminate the protein aggregates from affected individuals is an active area of research (Eisele et al., 2015). Much of our understanding of peptide and protein aggregation has been learned by studying the aggregation properties of β-amyloid and prion proteins, but it has been suggested that protein aggregation is an intrinsic property of polypeptide chains (Dobson, 2003).

A number of natural HDPs have been shown to oligomerize or aggregate, and it is possible that this tendency contributes to their antimicrobial activity and mechanism of action. For instance, the human cathelicidin peptide LL-37 has been shown to adopt an α-helical conformation in a salt-dependent manner (Johansson et al., 1998) and exists in an equilibrium between monomeric and oligomeric states, even at low peptide concentrations (Oren et al., 1999). These LL-37 oligomers persist in the presence of membranes and contribute to membrane instability (Bonucci et al., 2015), while amyloid-like fibrils have recently been reported for LL-37 mixed with liposomes

Peptide 2005 retained some of the anti-inflammatory activity seen for 1018, suppressing IL-1β levels by ~50% at a peptide concentration of 32.5 μM (Figure 6G). In contrast, 2002 and 2007 caused a significant increase in IL-1β levels from LPS-stimulated PBMCs (Figure 6G) consistent with previous conclusions that the peptide sequence requirements governing the suppression of pro-inflammatory signals are distinct from chemokine-inducing properties (Haney et al., 2015). All three of the non-toxic peptides suppressed the production of IL-6 from poly(I:C)-stimulated HBEs in a dose-dependent manner similar to the effects seen for 1018 (Figure 6H), suggesting that the anti-inflammatory activity of these peptides depends on the cell type and the kind of TLR agonist used to elicit an immune response. Altogether, the results from these immunomodulatory screens demonstrate that, in principle, it is possible to reduce the aggregation tendency of a synthetic HDP while retaining other favorable immunomodulatory properties.

A

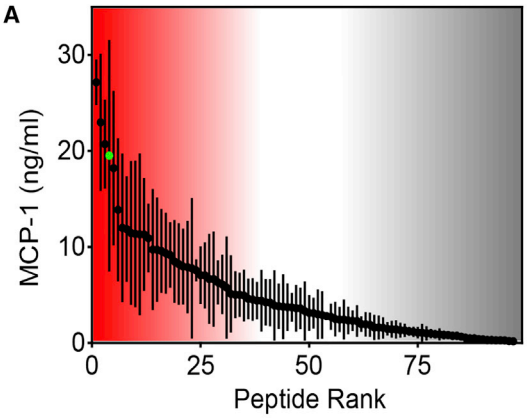

B

MCP-1	Sub. Amino Acid	1018 Sequence											
		V	R	L	I	V	A	V	R	I	W	R	R
Cationic	R	5.1	19.5	5.8	1.6	0.3	11.3	0.8	19.5	1.4	20.7	19.5	19.5
	K	3.6	12.0	3.6	3.1	3.3	27.2	3.0	11.9	0.3	6.7	9.6	8.2
Polar	Q	6.7	4.4	2.4	0.3	1.1	4.2	0.2	3.8	3.9	4.9	9.3	0.7
Small, Hydrophobic	G	23.0	13.9	2.5	0.5	1.1	6.3	1.6	1.3	1.0	1.2	7.6	0.7
	A	11.3	11.4	0.7	0.9	0.3	19.5	1.3	1.9	0.5	11.5	8.0	0.8
Large, Hydrophobic	W	2.0	0.4	7.1	2.3	1.6	2.3	2.9	0.3	5.0	19.5	0.4	3.8
	V	19.5	3.7	18.2	4.5	19.5	2.7	19.5	1.5	10.9	4.2	0.2	2.3
	L	3.7	1.9	19.5	7.0	4.4	7.8	3.1	0.5	7.9	5.0	1.4	2.4
	I	9.2	4.6	9.7	19.5	9.7	1.2	8.5	0.9	19.5	6.1	1.0	2.8

Figure 5. Ability of SPOT-Synthesized 1018 Derivatives to Stimulate MCP-1 Production from Human PBMCs

(A) The single amino acids substituted 1018 derivatives revealed differential ability to stimulate MCP-1 chemokine production from PBMCs. Each data point represents the average amount of MCP-1 (±SEM) induced by an individual 1018 derivative from three separate donors. The activity of SPOT-synthesized 1018 is shown in green.

(B) When mapped onto a substitution matrix, residues essential for chemokine induction become apparent, as well as those residues that could be mutated without negatively impacting the immunomodulatory activity of 1018. Peptides are colored from most active (top 25th percentile, red) to least active (bottom 75th percentile, gray).

composed of saturated phospholipids (Shahmiri et al., 2016). Interestingly, the β-amyloid protein has been shown to exhibit antibacterial activity *in vitro* (Soscia et al., 2010) and offered protection against *Salmonella typhimurium* infection in transgenic mice (Kumar et al., 2016), highlighting a potential biological role for this aggregation-prone peptide *in vivo*. Antibacterial activity has also been imparted to aggregation-prone sequences by introducing cationic residues into peptide sequences (Torrent et al., 2011), and it was recently suggested that synthetic peptides derived from aggregation-prone sequences of bacterial proteins could serve as a novel source of antibiotics (Bednarska et al., 2016).

Understanding the aggregation propensity of a peptide is an important consideration when evaluating a peptide for therapeutic use. Unfortunately, this characteristic is largely overlooked when the activity of a novel peptide sequence is reported. Many cationic peptides are highly soluble in water and likely remain soluble in assay conditions that evaluate antimicrobial activity (e.g., phosphate buffer). However, LL-37 loses its antibacterial potency under physiological salt concentrations (Bowdish et al., 2005), which highlights the possibility that different assay conditions can influence the activity of HDPs. Therefore, it is highly probable that, when a novel IDR peptide is identified or optimized under assay conditions that are not representative of the environment that would be encountered *in vivo*, this could lead to decreased potency or inactivity. In addition, aggregation of therapeutic proteins has been shown to elicit an immunogenic response that negatively impact on the safety and efficacy of protein-based drugs (Ratanji et al., 2014). Therefore, aggregation-prone peptides are typically discarded from consideration as drug candidates to avoid these potential pitfalls. However, if this aggregation property were to be characterized and understood, this could inform peptide design strategies to mitigate HDP aggregation.

Here we described the aggregation propensity of a synthetic HDP, 1018, and demonstrated that it is strongly influenced by the type of ion present in solution. Based on optical density measurements of 1 mg/mL 1018 prepared in solutions of various salts (Figure 2), an indicative order of anions that induced peptide aggregation is: phosphate ≈ benzoate ≈ nitrate > citrate > sulfate ≈ bicarbonate ≈ iodide ≈ chloride > acetate; and for cations: calcium > magnesium ≈ sodium ≈ potassium > guanidinium. This order largely follows the Hofmeister series of ions which was first described by Franz Hofmeister in 1888 based on the ability of an ion to affect protein solubility, with anions having a more pronounced effect than cations in general (Boström et al., 2005; Zhang and Cremer, 2006). The most effective salts for ''salting out,'' referred to as structure-makers or kosmotropes, display strong associations with water molecules and reduce the effective amount of water available to proteins, thus promoting aggregation. Conversely, the least-effective members, known as structure breakers or chaotropes, have weak water binding affinity, destabilize folded proteins by interacting with the amide portion of the polypeptide backbone, and increase the solubility of non-polar molecules (Marcus, 2009; Zhang and Cremer, 2006).

Our current hypothesis for how 1018 exerts its immunomodulatory activity is that, as soluble peptide is added to media, peptide monomers bind to and translocate into cells where they exert their immunomodulatory effects. This idea is based on the ability of HDPs to bind to biological membranes (Fjell et al., 2012), and preliminary studies have indicated that this peptide, like others, freely translocates across membranes and activates cells through a number of intracellular receptors (Mookherjee et al., 2009; Yu et al., 2009). At the same time, as soon as 1018

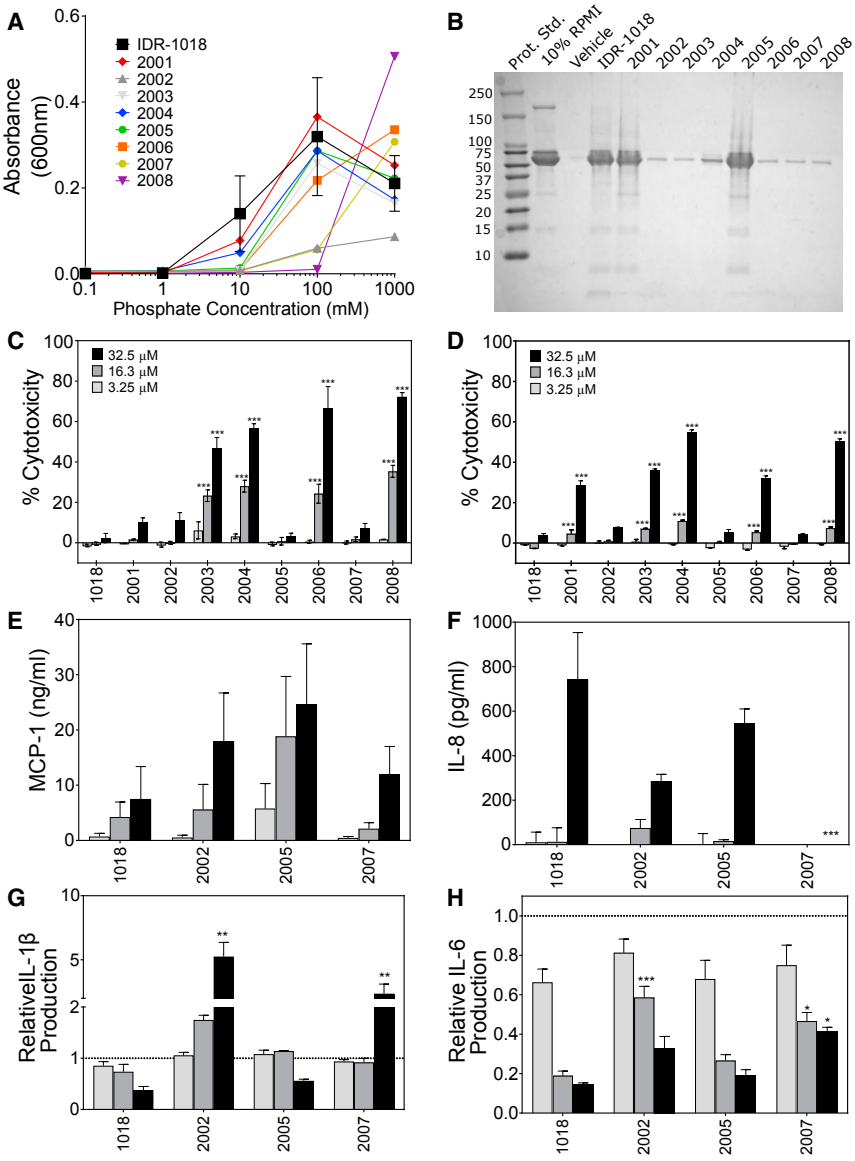

Figure 6. Activity of the Designed 1018 Derivatives

(A) Aggregation was evaluated by measuring the increase in sample turbidity at 600 nm of 1 mg/mL peptide solution prepared in increasing concentrations of sodium phosphate. Co-precipitation of serum proteins from media was evaluated by incubating 0.5 mg/mL peptide in 10% RPMI for 3 hr at 37°C followed by centrifugation to pellet any aggregates. The absorbance values for the 1018 samples represent the average of five individual measurements (±SD)

(B) The resuspended pellets were resolved on a 16% Tricine-SDS-PAGE gel and visualized with Coomassie stain.

(C and D) Peptide activity was evaluated at 32.5 (black), 16.25 (dark gray), and 3.25 μM (light gray), and cytotoxicity was evaluated against PBMCs (C) and HBEs (D) using the LDH release assay.

(E and F) Peptide-induced production of MCP-1 chemokines from PBMCs (E) or IL-8 from HBEs (F) was measured by ELISA.

(G and H) In addition, the peptide-mediated suppression of the pro-inflammatory cytokines IL-1β from LPS-stimulated PBMCs (G) or IL-6 from poly(I:C)-stimulated HBEs (H) was quantified and compared with the response of stimulated cells in the absence of peptide (defined as 1).

Data shown are mean ± SEM and only the immunomodulatory activity of non-toxic peptides is shown. Statistical significance was calculated using a two-way ANOVA with a Bonferroni correction comparing each derivative peptide treatment condition to the corresponding concentration of 1018. *$p \leq 0.05$, **$p \leq 0.01$, and ***$p \leq 0.001$. See also Figures S5 and S6.

is added to the tissue culture media, these conditions favor peptide aggregation, creating a balance of equilibrium states for the peptide monomers between those that interact with cells and those that will ultimately aggregate. Based on this model, it would be expected that pre-aggregating 1018 should reduce the number of monomers available to interact with cells leading to an overall reduction in the immunomodulatory activity. Having already identified conditions that promoted the self-assembly of 1018, we therefore sought to characterize the influence of aggregation on the immunomodulatory activity of 1018 *in vitro*.

When delivered from stock solutions prepared in non-aggregating stock solutions of saline or water, the immunomodulatory and cytotoxic activity profiles of 1018 were practically identical. However, when 1018 was delivered to PBMCs or HBEs in non-phosphate-containing aggregation-prone solutions, there was a definite shift in the immunomodulatory response compared with the peptide delivered in water. In general, the suppression of pro-inflammatory cytokines was decreased when PBMCs and HBEs were treated with pre-aggregated 1018, while the cytotoxicity and chemokine-inducing properties were enhanced. This is in agreement with previous studies that have demonstrated that aggregated proteins and peptides are toxic to cells (Bucciantini et al., 2002) and suggests that chemokine induction may be related to the toxic effect of aggregates, likely by stress-induced MAP kinase induction since this is influential in the immunomodulatory activity of peptides (Nijnik et al., 2010).

Unfortunately, all the 1018 samples were polydisperse under these aggregating conditions (as determined by dynamic light scattering, data not shown), indicating that there were no discrete peptide aggregates of a definable size. In addition, since we could not find conditions that prevented aggregation, we could not evaluate whether promoting 1018 monomers in solution could enhance the peptide activity *in vitro*. Importantly, two other peptides, IDR-1002 and IDR-HH2, were found to have distinct salt-specific aggregation properties compared with 1018 (Figure S4) despite strong sequence similarities among all three peptides. This suggested that a strong propensity to aggregate is not directly related to the immunomodulatory activity of a synthetic HDPs, and it therefore may be possible to modulate the aggregation property of

1018 by carefully manipulating the peptide sequence. Rationally designing peptide sequences to improve a specific property is common practice provided sufficient information is known regarding a particular structure-activity relationship. For instance, variants of human calcitonin with reduced aggregation propensities have been engineered using the sequence of poorly aggregating salmon calcitonin as a guide to inform specific mutations (Fowler et al., 2005). Unfortunately, the sequence requirements governing the immunomodulatory activities of IDR peptides are still poorly understood, making it difficult to rationally design 1018 variants without sacrificing some of the desirable peptide traits.

To identify the region of 1018 responsible for its aggregation tendency, a series of derivatives were synthesized with the goal of altering the highly hydrophobic stretch of amino acids between Leu-3 and Val-7, either by removing or shortening this hydrophobic stretch or by introducing a cationic Arg side chain or a Pro residue in this region (Table 1, 1101–1105). Hydrophobic surfaces in peptides are known to self-associate and drive the formation of aggregates (Kim and Hecht, 2006). As expected, all of these hydrophobic patch derivatives exhibited strongly reduced ''salting out'' tendencies compared with 1018 (Figure 4A), confirming that this region contributes to the self-assembly character of 1018. Unfortunately, all of these derivatives exhibited dramatically reduced immunomodulatory activity (Figures 4B–4G), demonstrating that this hydrophobic stretch also contributes to the biological activity of 1018.

A separate approach to engineer 1018 derivatives with decreased aggregation tendency was devised which employed the results from a recent immunomodulatory screen of single amino acid substitution variants of 1018 (Figure 5) to inform which residues could be manipulated in the parent sequence without sacrificing the biological activity. Most of these rationally designed 1018 derivatives involved mutating hydrophobic residues to cationic side chains with a particular emphasis on Ala-6 in the middle of the L^3IVAV^7 hydrophobic patch (Table 1, 2001–2008). Indeed, many of these derivatives exhibited decreased ''salting out'' tendencies compared with 1018 and most caused enhanced chemokine production from PBMCs and HBEs. Unfortunately, a number of these derivatives were unexpectedly toxic, underscoring the inherent difficulties associated with optimizing synthetic peptides for multiple activities (Haney et al., 2015).

The most active and non-toxic peptide from this set of rationally designed 1018 variants was peptide 2005 (A6R substitution in 1018). Peptide 2005 displayed low cytotoxicity, an enhanced ability to stimulate MCP-1 production from PBMCs, and retained much of the ability to suppress pro-inflammatory cytokines from PBMCs and HBEs (Figure 6). Interestingly, the aggregation property of 2005 was not completely abolished since this peptide still ''salted out'' at high phosphate concentrations and co-precipitated serum proteins from 10% RPMI. Nevertheless, this example demonstrates that it is possible to modulate the aggregation property of a synthetic IDR peptide without completely sacrificing the immunomodulatory activity.

Two other non-toxic 1018 derivatives with reduced aggregation tendencies were peptides 2002 and 2007. Importantly, both peptides did not co-precipitate serum proteins from tissue culture media, and they induced MCP-1 production from PBMCs and suppressed production of IL-6 from poly(I:C)-stimulated HBEs in a dose-dependent manner (Figure 6). However, some other immunomodulatory properties were reduced compared with 1018. Most notably, both peptides induced low IL-8 production from HBEs and caused an increase in IL-1β production from LPS-stimulated PBMCs. Taken together, these examples demonstrate that it is possible to engineer synthetic IDR peptides with reduced aggregation propensity, but focusing on preserving certain activities (e.g., chemokine induction) may have detrimental off-target effects on other biological properties. It should be noted that all of the 1018 derivatives were structurally characterized by circular dichroism spectroscopy in the presence of detergent micelles (Figure S6). While peptides 2002, 2005, and 2007 adopted similar conformations to 1018 in buffer and when bound to micelles, no consistent conclusions could be drawn regarding the conformational changes of all peptides and their observed immunomodulatory activity profiles. This suggests that the immunomodulatory activity of an IDR peptide is governed by the primary amino acid sequence as opposed to conformational plasticity of the peptide backbone or an ability to fold in membrane environments.

Understanding the basis of 1018 aggregation is critical for pharmaceutical development since solubility enhancement is usually a key step in the formulation process (Li and Zhao, 2007). It may be feasible to develop excipients for peptide delivery that are formulated to prevent peptide aggregation, thereby increasing the number of sequences that have therapeutic potential. Since many AMPs interact with biological membranes, lipid-based formulations have demonstrated potential in this regard (Zetterberg et al., 2011). Ultimately, a multi-pronged approach of rationally designing synthetic HDP derivatives coupled with a carefully selected formulation strategy will be necessary to translate the biological activities of HDPs to pharmaceutical applications.

SIGNIFICANCE

This original research article describes the anion-specific "salting out" effect of synthetic host defense peptides and postulates that this is a fundamental property of these peptides causing them to aggregate in solution. Here we demonstrate that the aggregation state of synthetic peptides directly impacts their immunomodulatory activity. Furthermore, our results reveal that it is possible to design peptides with reduced self-association tendency, while maintaining favorable immunomodulatory functions. This study highlights an important consideration that is often overlooked in peptide design strategies and is of value to researchers aiming to develop peptides for pharmaceutical applications.

STAR★METHODS

Detailed methods are provided in the online version of this paper and include the following:

- KEY RESOURCES TABLE
- CONTACT FOR REAGENT AND RESOURCE SHARING
- EXPERIMENTAL MODEL AND SUBJECT DETAILS
  - Peripheral Blood Mononuclear Cell (PBMC) Isolation
  - Human Bronchial Epithelial Cells

- METHOD DETAILS
  - Chemicals and Reagents
  - Peptide Synthesis
  - Peptide Aggregation Screen
  - Co-precipitation of Serum Proteins
  - Treatment of PBMCs
  - Treatment of Human Bronchial Epithelial Cells
  - Lactate Dehydrogenase Assay
  - Enzyme Linked Immunosorbent Assays
- QUANTIFICATION AND STATISTICAL ANALYSIS

SUPPLEMENTAL INFORMATION

Supplemental Information includes six figures and one table and can be found with this article online at http://dx.doi.org/10.1016/j.chembiol.2017.07.010.

AUTHOR CONTRIBUTIONS

Conceptualization, E.F.H. and R.E.W.H.; Methodology, E.F.H., B.W., and R.E.W.H.; Investigation and Formal Analysis, E.F.H., B.W., K.L., and A.L.H.; Writing – Original Draft, E.F.H.; Writing – Review & Editing, All Authors; Funding Acquisition, R.E.W.H.

ACKNOWLEDGMENTS

Thanks to Dr. Heidi Wolfmeier and Beverlie Baquir for reading early drafts of the manuscript. This work was supported by the Canadian Institutes of Health Research (CIHR) (funding reference number MOP-74493). The Jasco CD Spectropolarimeter was provided through grants from the Canadian Foundation for Innovation and the Michael Smith Foundation to the Laboratory of Molecular Biophysics. The peptides in this study were invented in part by E.F.H. and R.E.W.H., assigned to their employer the University of British Columbia, filed for patent protection, and licensed to ABT Innovations Inc. E.F.H and A.L.H. were recipients of postdoctoral fellowships from the CIHR. R.E.W.H. holds a Canada Research Chair and a UBC Killam Professorship.

Received: March 14, 2017
Revised: May 5, 2017
Accepted: July 7, 2017
Published: August 10, 2017

REFERENCES

Achtman, A.H., Pilat, S., Law, C.W., Lynn, D.J., Janot, L., Mayer, M.L., Ma, S., Kindrachuk, J., Finlay, B.B., Brinkman, F.S., et al. (2012). Effective adjunctive therapy by an innate defense regulatory peptide in a preclinical model of severe malaria. Sci. Transl. Med. *4*, 135ra64.

Aguzzi, A., and O'Connor, T. (2010). Protein aggregation diseases: pathogenicity and therapeutic perspectives. Nat. Rev. Drug Discov. *9*, 237–248.

Auvynet, C., El Amri, C., Lacombe, C., Bruston, F., Bourdais, J., Nicolas, P., and Rosenstein, Y. (2008). Structural requirements for antimicrobial versus chemoattractant activities for dermaseptin S9. FEBS J. *275*, 4134–4151.

Baets, G.D., Schymkowitz, J., and Rousseau, F. (2014). Predicting aggregation-prone sequences in proteins. Essays Biochem. *56*, 41–52.

Bednarska, N.G., van Eldere, J., Gallardo, R., Ganesan, A., Ramakers, M., Vogel, I., Baatsen, P., Staes, A., Goethals, M., Hammarström, P., et al. (2016). Protein aggregation as an antibiotic design strategy. Mol. Microbiol. *99*, 849–865.

Bolouri, H., Sävman, K., Wang, W., Thomas, A., Maurer, N., Dullaghan, E., Fjell, C.D., Ek, C.J., Hagberg, H., Hancock, R.E.W., et al. (2014). Innate defense regulator peptide 1018 protects against perinatal brain injury. Ann. Neurol. *75*, 395–410.

Bonucci, A., Caldaroni, E., Balducci, E., and Pogni, R. (2015). A spectroscopic study of the aggregation state of the human antimicrobial peptide LL-37 in bacterial versus host cell model membranes. Biochemistry *54*, 6760–6768.

Boström, M., Tavares, F.W., Finet, S., Skouri-Panet, F., Tardieu, A., and Ninham, B.W. (2005). Why forces between proteins follow different Hofmeister series for pH above and below pI. Biophys. Chem. *117*, 217–224.

Bowdish, D.M., Davidson, D.J., Lau, Y.E., Lee, K., Scott, M.G., and Hancock, R.E.W. (2005). Impact of LL-37 on anti-infective immunity. J. Leukoc. Biol. *77*, 451–459.

Bucciantini, M., Giannoni, E., Chiti, F., Baroni, F., Formigli, L., Zurdo, J., Taddei, N., Ramponi, G., Dobson, C.M., and Stefani, M. (2002). Inherent toxicity of aggregates implies a common mechanism for protein misfolding diseases. Nature *416*, 507–511.

Chiti, F., Stefani, M., Taddei, N., Ramponi, G., and Dobson, C.M. (2003). Rationalization of the effects of mutations on peptide and protein aggregation rates. Nature *424*, 805–808.

Conchillo-Solé, O., de Groot, N.S., Avilés, F.X., Vendrell, J., Daura, X., and Ventura, S. (2007). AGGRESCAN: a server for the prediction and evaluation of "hot spots" of aggregation in polypeptides. BMC Bioinformatics *8*, 65.

Darveau, R.P., and Hancock, R.E.W. (1983). Procedure for isolation of bacterial lipopolysaccharides from both smooth and rough *Pseudomonas aeruginosa* and *Salmonella typhimurium* strains. J. Bacteriol. *155*, 831–838.

Dobson, C.M. (2003). Protein folding and misfolding. Nature *426*, 884–890.

Doig, A.J., and Derreumaux, P. (2015). Inhibition of protein aggregation and amyloid formation by small molecules. Curr. Opin. Struct. Biol. *30*, 50–56.

Du, A.W., and Stenzel, M.H. (2014). Drug carriers for the delivery of therapeutic peptides. Biomacromolecules *15*, 1097–1114.

Eisele, Y.S., Monteiro, C., Fearns, C., Encalada, S.E., Wiseman, R.L., Powers, E.T., and Kelly, J.W. (2015). Targeting protein aggregation for the treatment of degenerative diseases. Nat. Rev. Drug Discov. *14*, 759–780.

Fjell, C.D., Hiss, J.A., Hancock, R.E.W., and Schneider, G. (2012). Designing antimicrobial peptides: form follows function. Nat. Rev. Drug Discov. *11*, 37–51.

Fowler, S.B., Poon, S., Muff, R., Chiti, F., Dobson, C.M., and Zurdo, J. (2005). Rational design of aggregation-resistant bioactive peptides: reengineering human calcitonin. Proc. Natl. Acad. Sci. USA *102*, 10105–10110.

Frokjaer, S., and Otzen, D.E. (2005). Protein drug stability: a formulation challenge. Nat. Rev. Drug Discov. *4*, 298–306.

de la Fuente-Núñez, C., Reffuveille, F., Haney, E.F., Straus, S.K., and Hancock, R.E.W. (2014). Broad-spectrum anti-biofilm peptide that targets a cellular stress response. PLoS Pathog. *10*, e1004152.

Ghosh, J.K., Shaool, D., Guillaud, P., Cicéron, L., Mazier, D., Kustanovich, I., Shai, Y., and Mor, A. (1997). Selective cytotoxicity of dermaseptin S3 toward intraerythrocytic plasmodium falciparum and the underlying molecular basis. J. Biol. Chem. *272*, 31609–31616.

Gruenert, D.C., Finkbeiner, W.E., and Widdicombe, J.H. (1995). Culture and transformation of human airway epithelial cells. Am. J. Physiol. *268*, L347–L360.

Hancock, R.E.W., Haney, E.F., and Gill, E.E. (2016). The immunology of host defence peptides: beyond antimicrobial activity. Nat. Rev. Immunol. *16*, 321–334.

Haney, E.F., Mansour, S.C., Hilchie, A.L., de la Fuente-Núñez, C., and Hancock, R.E.W. (2015). High throughput screening methods for assessing antibiofilm and immunomodulatory activities of synthetic peptides. Peptides *71*, 276–285.

Horn, M., Bertling, A., Brodde, M.F., Müller, A., Roth, J., Van Aken, H., Jurk, K., Heilmann, C., Peters, G., and Kehrel, B.E. (2012). Human neutrophil alpha-defensins induce formation of fibrinogen and thrombospondin-1 amyloid-like structures and activate platelets via glycoprotein IIb/IIIa. J. Thromb. Haemost. *10*, 647–661.

Johansson, J., Gudmundsson, G.H., Rottenberg, M.E., Berndt, K.D., and Agerberth, B. (1998). Conformation-dependent antibacterial activity of the naturally occurring human peptide LL-37. J. Biol. Chem. *273*, 3718–3724.

Kim, W., and Hecht, M.H. (2006). Generic hydrophobic residues are sufficient to promote aggregation of the Alzheimer's Aβ42 peptide. Proc. Natl. Acad. Sci. USA *103*, 15824–15829.

Kumar, D.K.V., Choi, S.H., Washicosky, K.J., Eimer, W.A., Tucker, S., Ghofrani, J., Lefkowitz, A., McColl, G., Goldstein, L.E., Tanzi, R.E., et al. (2016). Amyloid-β peptide protects against microbial infection in mouse and worm models of Alzheimer's disease. Sci. Transl. Med. *8*, 340ra72.

Li, P., and Zhao, L. (2007). Developing early formulations: practice and perspective. Int. J. Pharm. *341*, 1–19.

Li, Y., Li, X., Li, H., Lockridge, O., and Wang, G. (2007). A novel method for purifying recombinant human host defense cathelicidin LL-37 by utilizing its inherent property of aggregation. Protein Expr. Purif. *54*, 157–165.

Mansour, S.C., de la Fuente-Núñez, C., and Hancock, R.E.W. (2015). Peptide IDR-1018: modulating the immune system and targeting bacterial biofilms to treat antibiotic-resistant bacterial infections. J. Pept. Sci. *21*, 323–329.

Marcus, Y. (2009). Effect of ions on the structure of water: structure making and breaking. Chem. Rev. *109*, 1346–1370.

Mookherjee, N., Lippert, D.N., Hamill, P., Falsafi, R., Nijnik, A., Kindrachuk, J., Pistolic, J., Gardy, J., Miri, P., Naseer, M., et al. (2009). Intracellular receptor for human host defense peptide LL-37 in monocytes. J. Immunol. *183*, 2688–2696.

Morimoto, A., Irie, K., Murakami, K., Ohigashi, H., Shindo, M., Nagao, M., Shimizu, T., and Shirasawa, T. (2002). Aggregation and neurotoxicity of mutant amyloid β (Aβ) peptides with proline replacement: importance of turn formation at positions 22 and 23. Biochem. Biophys. Res. Commun. *295*, 306–311.

Nguyen, L.T., Haney, E.F., and Vogel, H.J. (2011). The expanding scope of antimicrobial peptide structures and their modes of action. Trends Biotechnol. *29*, 464–472.

Nijnik, A., Madera, L., Ma, S., Waldbrook, M., Elliott, M.R., Easton, D.M., Mayer, M.L., Mullaly, S.C., Kindrachuk, J., Jenssen, H., et al. (2010). Synthetic cationic peptide IDR-1002 provides protection against bacterial infections through chemokine induction and enhanced leukocyte recruitment. J. Immunol. *184*, 2539–2550.

Niyonsaba, F., Madera, L., Afacan, N., Okumura, K., Ogawa, H., and Hancock, R.E.W. (2013). The innate defense regulator peptides IDR-HH2, IDR-1002, and IDR-1018 modulate human neutrophil functions. J. Leukoc. Biol. *94*, 159–170.

Oren, Z., Lerman, J.C., Gudmundsson, G.H., Agerberth, B., and Shai, Y. (1999). Structure and organization of the human antimicrobial peptide LL-37 in phospholipid membranes: relevance to the molecular basis for its non-cell-selective activity. Biochem. J. *341*, 501–513.

Pena, O.M., Afacan, N., Pistolic, J., Chen, C., Madera, L., Falsafi, R., Fjell, C.D., and Hancock, R.E.W. (2013). Synthetic cationic peptide IDR-1018 modulates human macrophage differentiation. PLoS One *8*, e52449.

Ratanji, K.D., Derrick, J.P., Dearman, R.J., and Kimber, I. (2014). Immunogenicity of therapeutic proteins: influence of aggregation. J. Immunotoxicol *11*, 99–109.

Richardson, J.S., and Richardson, D.C. (1989). Principles and patterns of protein conformation. In Prediction of Protein Structure and the Principles of Protein Conformation, G.D. Fasman, ed. (Springer), pp. 1–98.

Rivas-Santiago, B., Castañeda-Delgado, J.E., Santiago, C.E.R., Waldbrook, M., González-Curiel, I., León–Contreras, J.C., Enciso-Moreno, J.A., del Villar, V., Mendez-Ramos, J., Hancock, R.E.W., et al. (2013). Ability of innate defence regulator peptides IDR-1002, IDR-HH2 and IDR-1018 to protect against *Mycobacterium tuberculosis* infections in animal models. PLoS One *8*, e59119.

Roberts, C.J. (2014). Therapeutic protein aggregation: mechanisms, design, and control. Trends Biotechnol. *32*, 372–380.

Sarig, H., Rotem, S., Ziserman, L., Danino, D., and Mor, A. (2008). Impact of self-assembly properties on antibacterial activity of short acyl-lysine oligomers. Antimicrob. Agents Chemother. *52*, 4308–4314.

Schägger, H. (2006). Tricine-SDS-PAGE. Nat. Protoc. *1*, 16–22.

Shahmiri, M., Enciso, M., Adda, C.G., Smith, B.J., Perugini, M.A., and Mechler, A. (2016). Membrane core-specific antimicrobial action of cathelicidin LL-37 peptide switches between pore and nanofibre formation. Sci. Rep. *6*, 38184.

Soscia, S.J., Kirby, J.E., Washicosky, K.J., Tucker, S.M., Ingelsson, M., Hyman, B., Burton, M.A., Goldstein, L.E., Duong, S., Tanzi, R.E., et al. (2010). The Alzheimer's disease-associated amyloid β-protein is an antimicrobial peptide. PLoS One *5*, e9505.

Steinstraesser, L., Hirsch, T., Schulte, M., Kueckelhaus, M., Jacobsen, F., Mersch, E.A., Stricker, I., Afacan, N., Jenssen, H., Hancock, R.E.W., et al. (2012). Innate defense regulator peptide 1018 in wound healing and wound infection. PLoS One *7*, e39373.

Torrent, M., Valle, J., Nogues, M.V., Boix, E., and Andreu, D. (2011). The generation of antimicrobial peptide activity: a trade-off between charge and aggregation? Angew. Chem. Int. Ed. *50*, 10686–10689.

Wieczorek, M., Jenssen, H., Kindrachuk, J., Scott, W.R., Elliott, M., Hilpert, K., Cheng, J.T., Hancock, R.E.W., and Straus, S.K. (2010). Structural studies of a peptide with immune modulating and direct antimicrobial activity. Chem. Biol. *17*, 970–980.

Yu, H.B., Kielczewska, A., Rozek, A., Takenaka, S., Li, Y., Thorson, L., Hancock, R.E.W., Guarna, M.M., North, J.R., Foster, L.J., et al. (2009). Sequestosome-1/p62 is the key intracellular target of innate defense regulator peptide. J. Biol. Chem. *284*, 36007–36011.

Zetterberg, M.M., Reijmar, K., Pränting, M., Engström, Å., Andersson, D.I., and Edwards, K. (2011). PEG-stabilized lipid disks as carriers for amphiphilic antimicrobial peptides. J. Controlled Release *156*, 323–328.

Zhang, Y., and Cremer, P.S. (2006). Interactions between macromolecules and ions: the Hofmeister series. Curr. Opin. Chem. Biol. *10*, 658–663.

STAR★METHODS

KEY RESOURCES TABLE

REAGENT or RESOURCE	SOURCE	IDENTIFIER
Antibodies		
IL-1 beta Monoclonal Antibody (CRM56)	eBioscience	14-7018-85
IL-1 beta Monoclonal Antibody (CRM57), Biotin	eBioscience	13-7016-85
CCL2 (MCP-1) Monoclonal Antibody (5D3-F7)	eBioscience	14-7099-85
CCL2 (MCP-1) Monoclonal Antibody (2H5), Biotin	eBioscience	13-7096-85
IL-6 Monoclonal Antibody	eBioscience	14-7069-85
IL-6 Monoclonal Antibody, Biotin	eBioscience	13-7068-85
CXCL8 (IL-8) Monoclonal Antibody	Invitrogen	AHC0982
CXCL8 (IL-8) Monoclonal Antibody, Biotin	Invitrogen	AHC0789
Avidin HRP	eBioscience	18-4100-51
Biological Samples		
Peripheral blood mononuclear cells (PBMCs)	Healthy donors	N/A
Chemicals, Peptides, and Recombinant Proteins		
IDR-1018 (VRLIVAVRIWRR-NH2), >95% Pure	CPC Scientific	N/A
IDR-1002 (VQRWLIVWRIRK-NH2), >95% Pure	CPC Scientific	N/A
IDR-HH2 (VQLRIRVAVIRA -NH2), >95% Pure	CPC Scientific	N/A
1101 (VRRIWRR-NH2), >90% Pure	21st Century Biochemicals	N/A
1102 (VRFRIWRR-NH2), >90% Pure	21st Century Biochemicals	N/A
1103 (VRVAVRIWRR-NH2), >90% Pure	21st Century Biochemicals	N/A
1104 (VRLIPAVRIWRR-NH2), >90% Pure	21st Century Biochemicals	N/A
1105 (VRLIRAVRIWRR-NH2), >90% Pure	21st Century Biochemicals	N/A
2001 (VRLIVKVRIWRR-NH2), >95% Pure	Genscript	N/A
2002 (VRLIVAVRIRRR-NH2), >95% Pure	Genscript	N/A
2003 (VRLIVKVRIRRR-NH2), >95% Pure	Genscript	N/A
2004 (VRVIVKVRIRRR-NH2), >95% Pure	Genscript	N/A
2005 (VRLIVRVRIWRR-NH2), >95% Pure	Genscript	N/A
2006 (VRWIVKVRIRRR-NH2), >95% Pure	Genscript	N/A
2007 (RRLIVKVRIWRR-NH2), >95% Pure	Genscript	N/A
2008 (RRWIVKVRIRRR-NH2), >95% Pure	Genscript	N/A
SPOT-synthesized IDR-1018 derivative array on cellulose sheet	Kinexus Inc.	N/A
MCP-1 (MCAF) Recombinant Human Protein (ELISA Standard)	R&D Systems	279-MC
Human IL-1 beta Recombinant Protein	eBioscience	BMS331
Human IL-6 Recombinant Protein	eBioscience	14-8069-62
IL-8 Monocyte Recopmbinant Human Protein	Life Technologies	PHC0884
Critical Commercial Assays		
Cytotoxicity Detection Kit (LDH)	Roche	11644793001
1X TMB ELISA Substrate Solution	eBioscience	00-4201-56
ELISA stop solution (2.0N Sulfuric Acid, Solution)	VWR	BDH7500-1
Experimental Models: Cell Lines		
Simian virus 40 transformed immortalized HBE cell line (16HBE14O-)	Gruenert et al., 1995	N/A
Software and Algorithms		
GraphPad Prism, Version 7.01	GraphPad Software, Inc.	https://www.graphpad.com/
AGGRESCAN – The Hot Spot Finder	Conchillo-Solé et al., 2007	http://bioinf.uab.es/aggrescan/

(*Continued on next page*)

Continued

REAGENT or RESOURCE	SOURCE	IDENTIFIER
Other		
P. aeruginosa, PAO1, purified LPS	Darveau and Hancock, 1983	http://cmdr.ubc.ca/bobh/method/lps-isolation-darveau-hancock-method/
polyinosinic : polycytidylic acid (poly I:C)	Invivogen	31852-29-6
Sodium heparin blood collection tubes	BD Biosciences	366480
Lymphoprep™	STEMCELL Technologies	7851
RPMI-1640 Medium (+25mM HEPES, +L-Glutamine)	GE Healthcare	SH30255.01
Minimum essential medium, MEM	ThermoFisher (Gibco)	11090081
Phosphate-buffered saline, pH 7.4	ThermoFisher (Gibco)	10010023
Fetal Bovine Serum, FBS	ThermoFisher (Gibco)	12483-020
Trypsin-EDTA (0.25%)	ThermoFisher (Gibco)	25200-056
L-Glutamine	ThermoFisher (Gibco)	25030-081

CONTACT FOR REAGENT AND RESOURCE SHARING

Further information and requests for resources and reagents should be directed to the lead contact, Dr. Robert E. W. Hancock (bob@hancocklab.com).

EXPERIMENTAL MODEL AND SUBJECT DETAILS

Peripheral Blood Mononuclear Cell (PBMC) Isolation

Blood from healthy and consenting human volunteers (both male and female) was collected in sodium heparin anticoagulant collection tubes (BD Biosciences, Franklin Lakes, NJ), in accordance with the University of British Columbia ethics guidelines. The blood was diluted in an equal volume of PBS buffer (pH 7.0) then layered onto Lymphoprep density gradient medium (STEMCELL Technologies Inc. Vancouver, BC) and centrifuged at ~500 x *g* for 20 minutes in an Allegra 6 centrifuge (Beckman-Coulter, Brea, CA). The buffy coat was collected from the centrifuged samples, and PBMCs were washed three times with PBS and resuspended in 10% RPMI. Cell density was determined using Turks staining of a diluted sample of purified cells followed by counting using a hemacytometer.

Human Bronchial Epithelial Cells

Simian virus 40 transformed immortalized human bronchial epithelial (HBE) cells (16HBE14o-), kindly obtained from Dr. D. Gruenert (University of California San Francisco) (Gruenert et al., 1995), were grown at 37°C with 5% CO_2 in tissue culture treated flasks containing MEM media supplemented with 10% FBS (10% MEM) and 2 mM L-glutamine. HBE cells were grown until the monolayer of cells reached 80-90% confluence, refreshing the media as required. The 16HBE14o- cell line is male and this particular cell line has not been authenticated at this time.

METHOD DETAILS

Chemicals and Reagents

Roswell Park Memorial Institute (RPMI) 1640 medium was purchased from GE Healthcare (Chicago, IL) while all other media and tissue culture reagents such as minimum essential medium (MEM) and phosphate-buffered saline (PBS) were purchased from Gibco, ThermoFisher (Pittsburgh, PA). All other chemicals and reagents were purchased from Sigma-Aldrich (St. Louis, MO) or ThermoFisher unless otherwise indicated.

Peptide Synthesis

IDR-1018, IDR-1002 and IDR-HH2 were synthesized by CPC Scientific Inc. (Sunnyvale, CA) and obtained at >95% purity. The truncated versions of 1018 (peptides 1101-1103) as well as V5P (1104) and V5R (1105) were synthesized by 21st Century Biochemicals (Marlboro, MA) and obtained at >90% purity. The rationally designed 1018 variants (peptides 2001-2008) were synthesized by Genscript (Piscataway, NJ) to >95% purity. The SPOT-synthesized peptide array on cellulose sheets consisting of single amino acids substitution variants of 1018 was obtained from Kinexus Inc. (Vancouver, BC, Canada). The online tool, AGGRESCAN (Conchillo-Solé et al., 2007) was used to predict the aggregation propensity of the synthetic peptides. The names, sequences and physicochemical properties of all the purified peptides (>90%) used in this study are summarized in Table 1.

Peptide Aggregation Screen

Stock solutions of 1018 and derivatives thereof were prepared at 10 mg/ml in water and subsequently diluted into different excipient solutions (a complete list is shown in Table S1). Samples were mixed in clear 96-well flat-bottom plates (Greiner Bio-One, Kremsmünster, Austria) to a final peptide concentration of 1 mg/ml and a sample volume of 100 μl. Water was added into each vehicle in parallel to serve as a negative control. Following overnight incubation at 20°C, the optical density at 600nm (OD_{600}) of each sample was recorded on a PowerWave X 340 microplate reader (Bio-Tek Instruments Inc., Winooski, VT). The peptide was considered to aggregate if a specific condition led to an increase in sample turbidity/OD_{600} relative to the negative control.

Co-precipitation of Serum Proteins

Peptide was incubated in 50 μl RPMI media supplemented with 10% (v/v) heat inactivated fetal bovine serum (10% RPMI) at a specific peptide concentration. Following incubation, each sample was centrifuged at 21 100 x *g* on a Sorvall Legend Micro 21R bench top centrifuge and the supernatant was aspirated, leaving any pelleted proteins at the bottom of the microfuge tube. The pellet was resuspended in 10 μl of water. Samples of supernatant or resuspended pellet were diluted 1:1 in 2X gel loading buffer (125 mM Tris-HCl, pH 6.8; 20% glycerol; 4% SDS; 4% β-mercaptoethanol; 0.1% bromophenol blue), boiled at 100°C for 5 minutes and then loaded onto a polyacrylamide gel. The protein bands were resolved on either a 12% SDS-PAGE gel for the 1018 concentration dependence experiment, or a Tricine-SDS-PAGE gel (Schägger, 2006) for evaluating the aggregation propensity of the 1018 derived peptides, 2001-2008. The gels were stained with 0.1% Coomassie blue dye in 10% (v/v) acetic acid and 50% (v/v) methanol, and then subsequently destained in a solution containing 20% (v/v) ethanol and 7.5% (v/v) acetic acid. The gels were visualized on a Chemi Genius 2 Bio Imaging System (Syngene, Cambridge, UK).

Treatment of PBMCs

Isolated PBMCs were seeded in Costar 96-well flat bottom tissue culture treated plates (Corning Inc., Corning, NY) by placing, into each well, 50 μl of cells at a concentration of 2 x 10^6 cells/ml in 10% RPMI media. The cells were allowed to rest for one hour followed by treatment with peptide in the absence or presence of 10 ng/ml *P. aeruginosa* PAO1 lipopolysaccharide (LPS). LPS was purified in-house according to the protocol described in (Darveau and Hancock, 1983). Peptide stock solutions at 1 mg/ml were prepared in each of the different vehicles (water, sterile saline solution, 10% RPMI, filter sterilized solutions of 200 mM $NaNO_3$ or Na_2SO_4, PBS, or filter sterilized 200 mM Na_2HPO_4 at pH 7.0) from a stock peptide solution of 10 mg/ml prepared in endotoxin free water. These 1 mg/ml solutions were immediately further diluted to 10X the final peptide concentration in their appropriate vehicle and 10 μl was added to 90 μl of media containing PBMCs either with or without LPS. For the SPOT-synthesized peptide samples, each peptide was solubilized in 200 μl of sterile water and 10 μl of the resulting peptide stock solution (~200 μM) was added directly to 90 μl of PBMCs. The final volume in each well was 100 μl and the final cell density was 1 x 10^6 cells/ml after additives. After overnight incubation at 37°C and 5% CO_2, the cells were visualized at 10X magnification on a Nikon Eclipse TS100 microscope. The plates were then spun at ~400 x *g* in an Allegra 6 centrifuge, and the supernatants were transferred to sterile 96-well polypropylene plates for subsequent lactate dehydrogenase (LDH) assay, which was run immediately, or frozen at -20°C for future ELISA analysis (see below).

Treatment of Human Bronchial Epithelial Cells

Cultures of HBE cells that had reached 80-90% confluence were detached from their growth flask by treatment with trypsin-EDTA for 5 minutes. The detached cells were pelleted by low speed centrifugation and then resuspended in 10% MEM. HBE cells (200 μl in 10% MEM) were seeded at 4-5 X 10^4 cells/well in a 96-well flat-bottom tissue culture treated polystyrene plate. The HBE cells were then grown overnight at 37°C with 5% CO_2, allowing the cells to adhere and reach confluence. The following day, the 10% MEM medium was aspirated and the cells were rinsed with 200 μl of MEM media containing 2 mM L-glutamine and 1% FBS (1% MEM). Finally, 100 μl of 1% MEM media was added to each well and the cells were rested for one hour. After resting, the cells were treated with peptide or vehicle control (20 μl) in the presence or absence of 100 ng/ml polyinosinic:polycytidylic acid (pI:C; Invivogen, San Diego, CA). Peptide stock solutions were prepared as described for the treatment of PBMCs (except the media sample was prepared in 1% MEM instead of 10% RPMI) and the final volume in each well was 200 μl. The HBE samples were incubated overnight at 37°C with 5% CO_2 and the following day, supernatants were collected into 96-well polypropylene plates for LDH assay and ELISA analysis.

Lactate Dehydrogenase Assay

The cytotoxicity of the peptides against PBMCs and HBEs was evaluated with the Cytotoxicity Detection Kit (Roche Diagnostics, Basel, Switzerland), which measures the enzyme activity of LDH released from damaged cells. Supernatants of cells treated with an equivalent volume of diluent or lysed by adding 2% Triton-X100 to the cells one hour prior to collecting the sample supernatants, served as the negative (0% toxicity) and positive controls (100% toxicity), respectively. LDH assays were carried out on at least 3 separate biological replicates for both PBMC and HBE samples.

Enzyme Linked Immunosorbent Assays

Enzyme linked immunosorbent assays (ELISA) kits from eBioscience Inc. (San Diego, CA) or Invitrogen (Carlsbad, CA) were used to quantify the levels of Monocyte Chemotactic Protein 1 (MCP-1) and Interleukin (IL)-8 produced by peptide treated PBMCs and HBEs respectively. Additionally, the levels of the pro-inflammatory cytokine IL-1β were assessed for LPS-stimulated PBMCs in

the presence of peptide. For HBE cells, IL-6 served as a pro-inflammatory cytokine marker in cells stimulated with pI:C. All ELISAs were carried out on at least three separate biological replicates.

QUANTIFICATION AND STATISTICAL ANALYSIS

All data was plotted and analyzed using GraphPad Prism, version 7.01 (GraphPad Software, La Jolla, CA). Statistical significance in the immunomodulatory assays was calculated in GraphPad using a two-way ANOVA with a Bonferonni correction comparing each derivative peptide treatment condition to the corresponding concentration of 1018 (* denotes p-value $\leq$ 0.05, ** p-value $\leq$ 0.01 and *** p-value $\leq$ 0.001).